Supporting Information

Enhanced Electrocatalytic Nitrogen Reduction Activity by Incorporation of Carbon Layer on SnS Microflowers

Weikang Yu,[1,2] Fenghao Shu,[1] Yifeng Huang,[1] Fangqi Yang,[1] Qiangguo Meng,[1] Zhi Zou,[1] Jun Wang,[1*] Zheling Zeng,[1] Guifu Zou,[2] Shuguang Deng [3*]

W. K. Yu, F. H. Shu, Y. f. Huang, F. Q. Yang, S. Zhu, Q. G. Meng, Z. Zou, Prof. J. Wang, Prof. Q. Deng, Prof. Z. L. Zeng, Prof. S. G. Deng

School of Resource, Environmental and Chemical Engineering, Nanchang University, No. 999 Xuefu Avenue, Jiangxi 330031, PR China

E-mail: jwang7@ncu.edu.cn (J. Wang)

E-mail: shuguang.deng@asu.edu (S. Deng)

W. K. Yu, Prof. G. F. Zou

Soochow Institute for Energy and Materials Innovations & Key Laboratory of Advanced Carbon Materials and Wearable Energy Technologies of Jiangsu Province, Soochow University, Suzhou 215006, PR China.

Prof. S. G. Deng

School for Engineering of Matter, Transport and Energy, Arizona State University, 551 E.Tyler Mall, Tempe, AZ 85287, USA

*Corresponding author:

E-mail: jwang7@ncu.edu.cn (J. Wang);

E-mail: shuguang.deng@asu.edu (S. Deng)

Table of contents

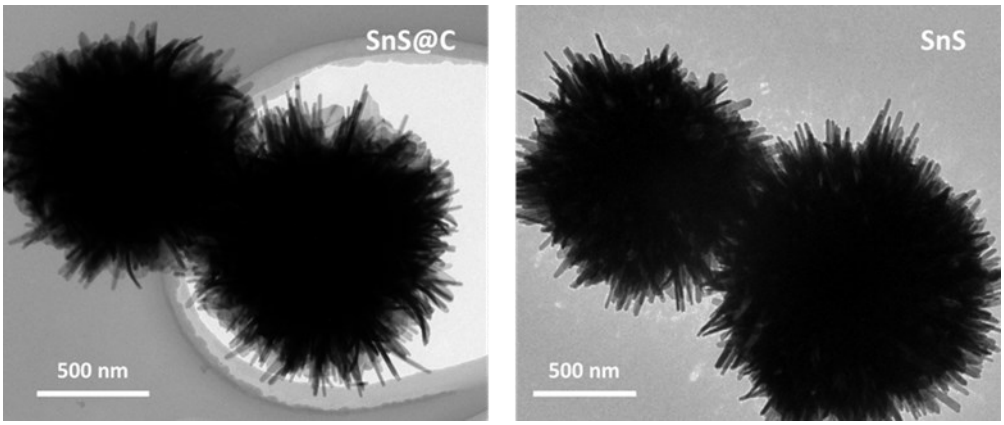

Figure S1. TEM images of SnS@C and SnS microflowers.

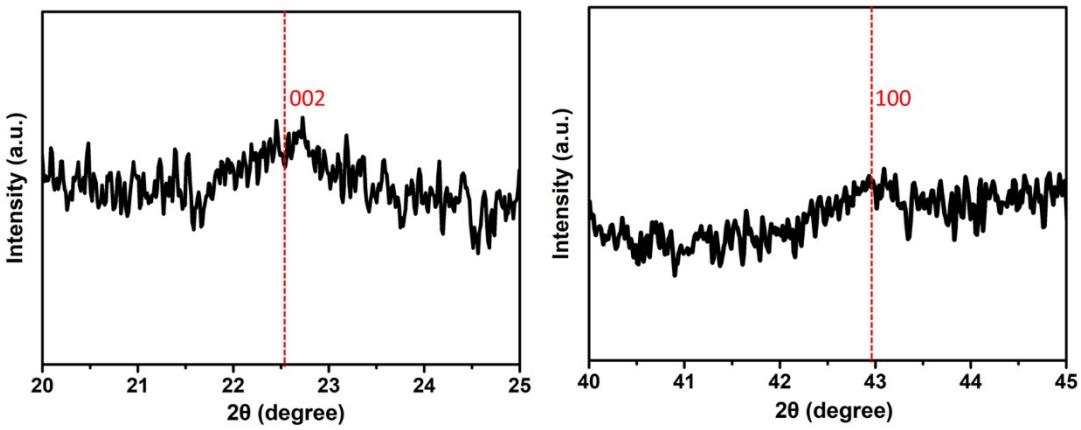

Figure S2. XRD patterns of SnS@C.

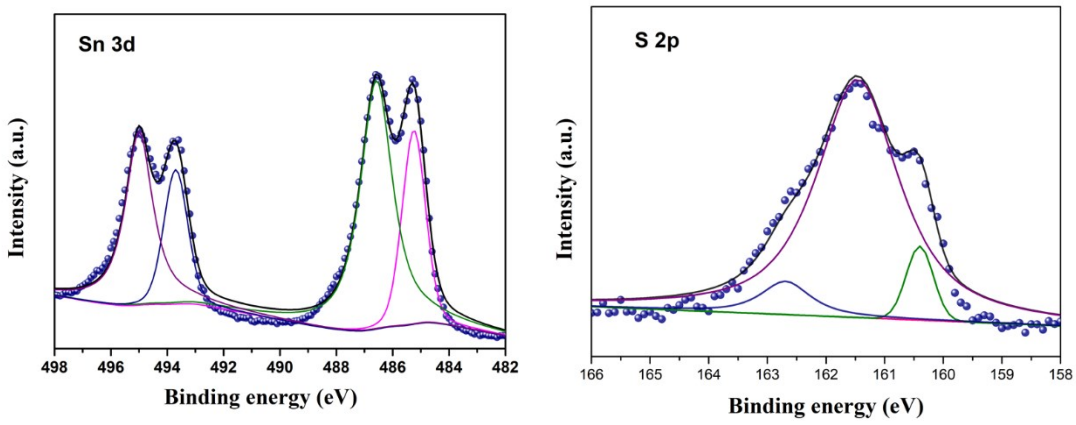

86

87 **Figure S3.** High-resolution XPS spectra of Sn 3d and S 2p on SnS.

88

89

90

91

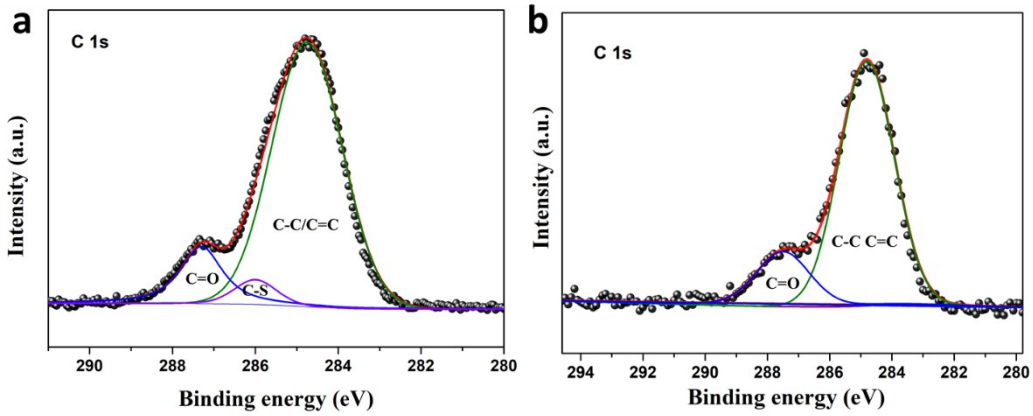

92

93 **Figure S4.** High-resolution XPS spectra of C 1s of a) SnS@C and b) SnS.

94

95

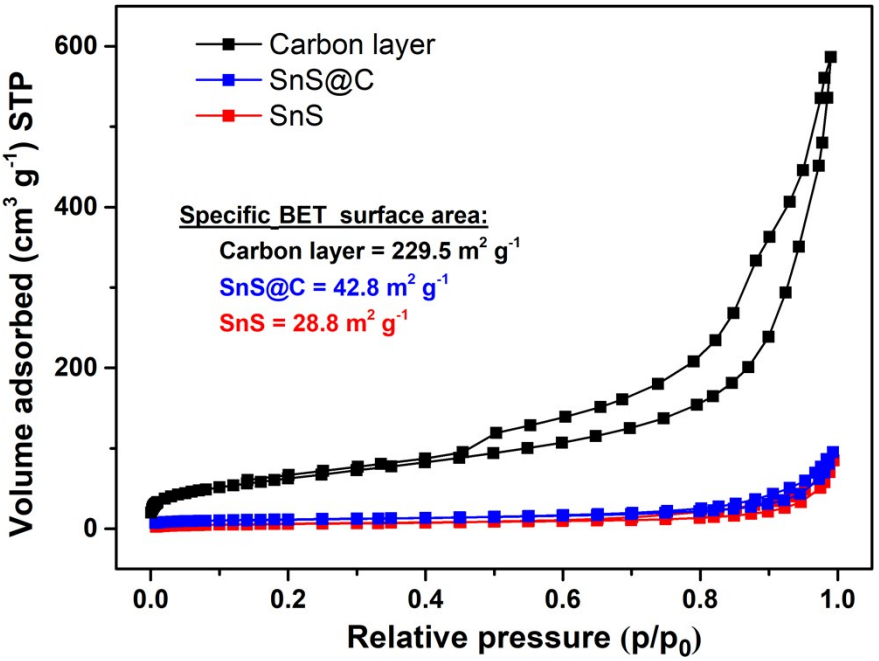

Figure S5. N_2 adsorption-desorption isotherms of the carbon layer, SnS@C, and SnS at 77 K.

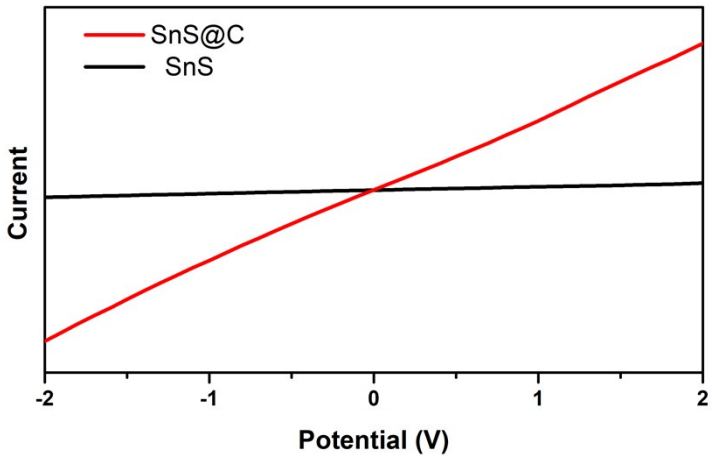

Figure S6. I-U curves of SnS@C and SnS at room temperature.

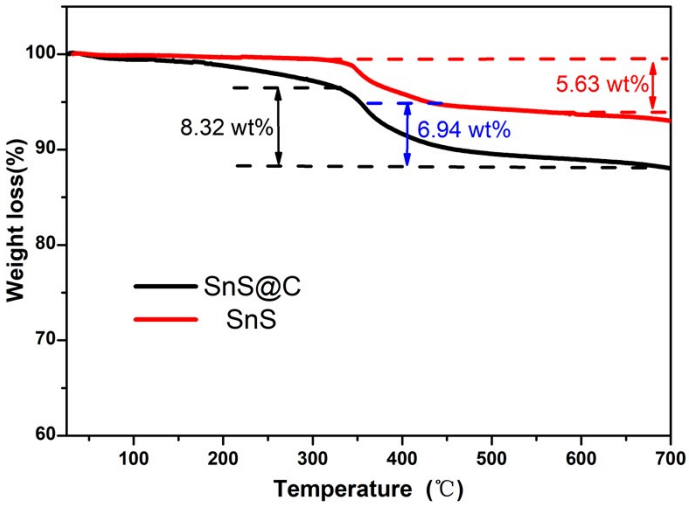

Figure S7. TGA curves of SnS@C and SnS under an Ar-air atmosphere.

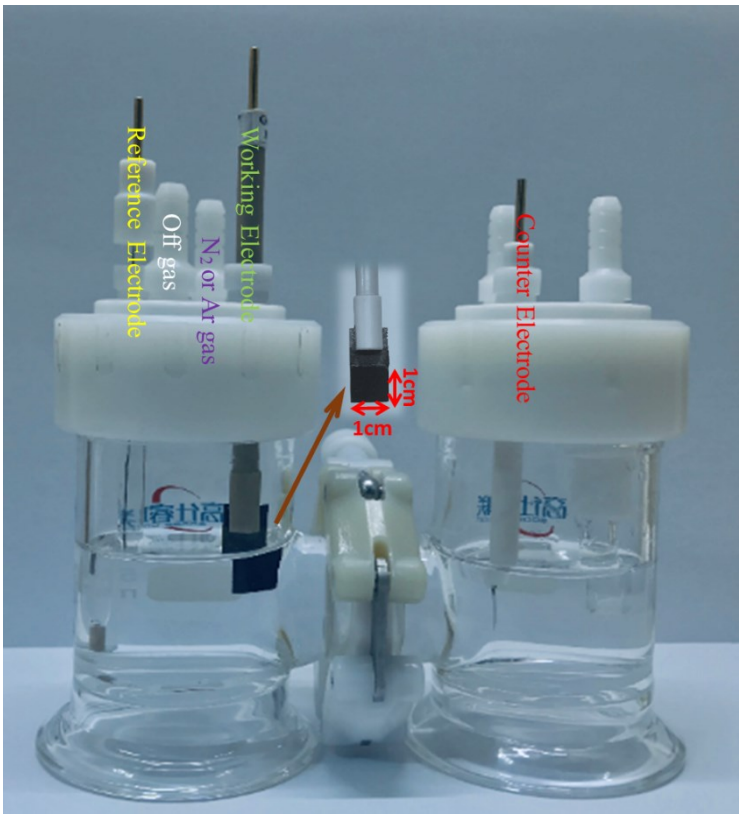

114

115 **Figure S8.** Optical photograph of the gas-tight three-electrode configured two-
116 compartment electrochemical cell.

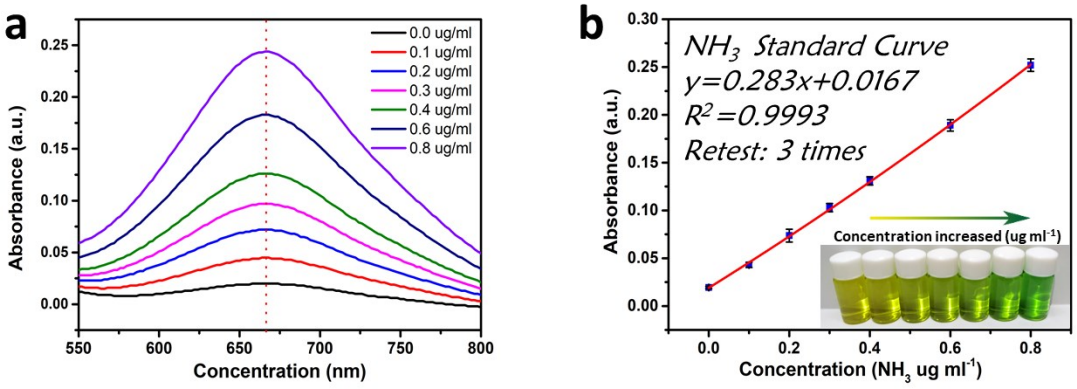

117

Figure S9. Determination of the produced ammonia in 0.1 M Na_2SO_4. (a) UV-Vis absorption spectra of various NH_3 concentrations after avoid light incubated for 1 h at room temperature. (b) Corresponding calibration curves for the colorimetric NH_3 assay using the indophenol blue method.

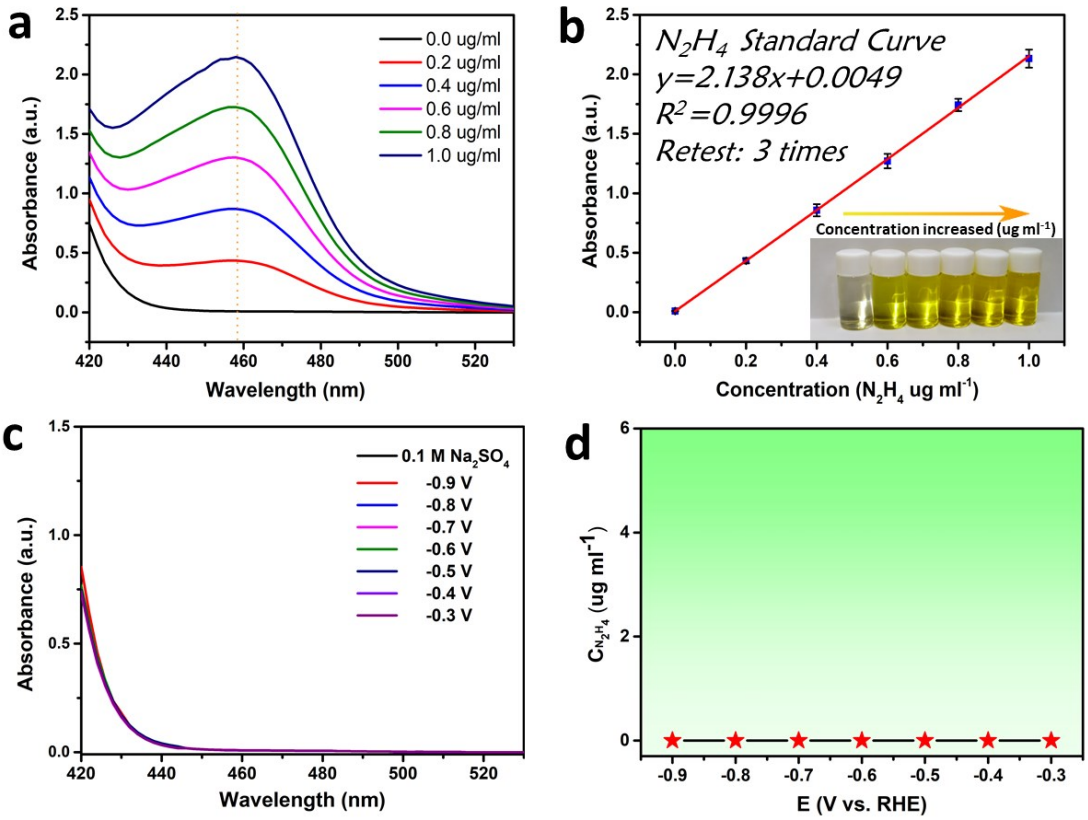

Figure S10. Determination of the produced hydrazine in 0.1 M Na_2SO_4. (a) UV-Vis absorption spectra of various N_2H_4 concentrations after incubated for 20 min at room temperature. (b) Corresponding calibration curves for the colorimetric N_2H_4 assay using the Watt-Chrisp method. (c) UV-Vis absorption spectra of the electrolytes stained with the Watt-Chrisp method before and after 7200s electrolysis at a series of potentials using SnS@C as the working electrode. (d) N_2H_4 concentrations at corresponding potentials.

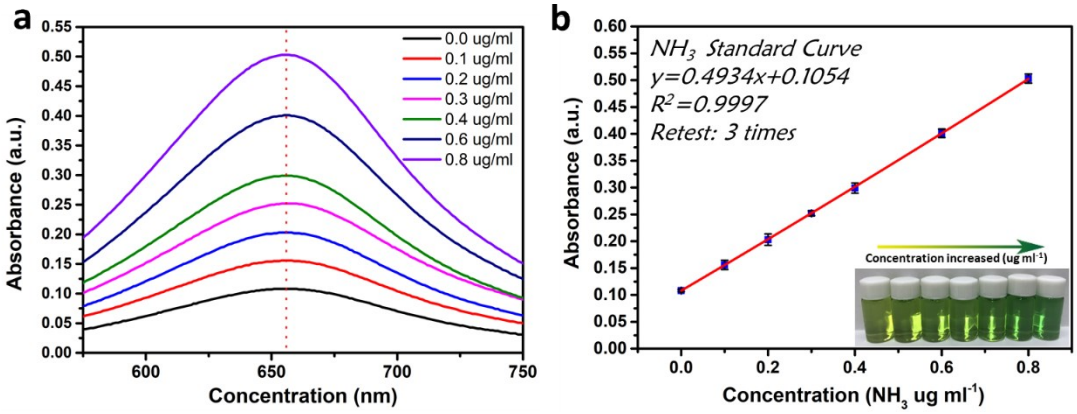

Figure S11. Determination of the produced ammonia in 0.1 M HCl. (a) UV-Vis absorption spectra of various NH_3 concentrations after avoid light incubated for 2 h at room temperature. (b) Corresponding calibration curves for the colorimetric NH_3 assay using the indophenol blue method.

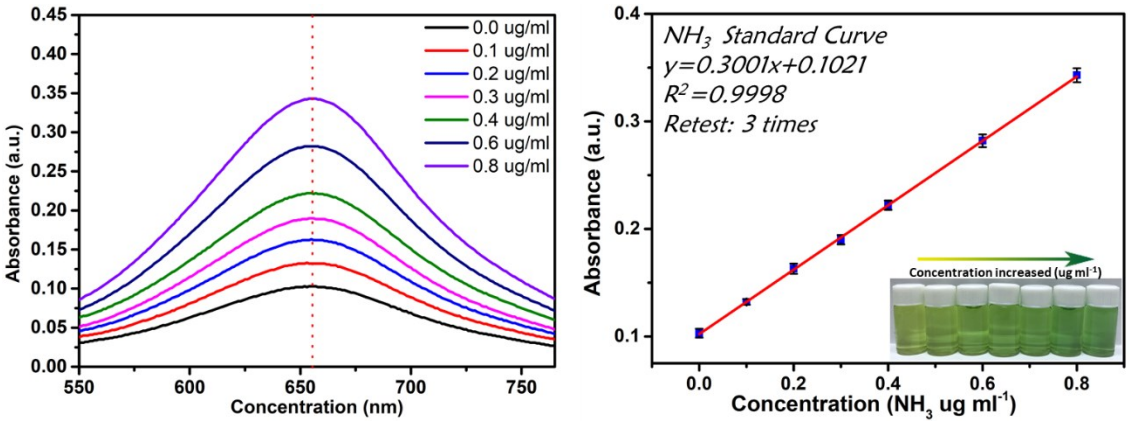

Figure S12. Determination of the produced ammonia in 0.1 M KOH. (a) UV-Vis absorption spectra of various NH_3 concentrations after avoid light incubated for 2 h at room temperature. (b) Corresponding calibration curves for the colorimetric NH_3 assay using the indophenol blue method.

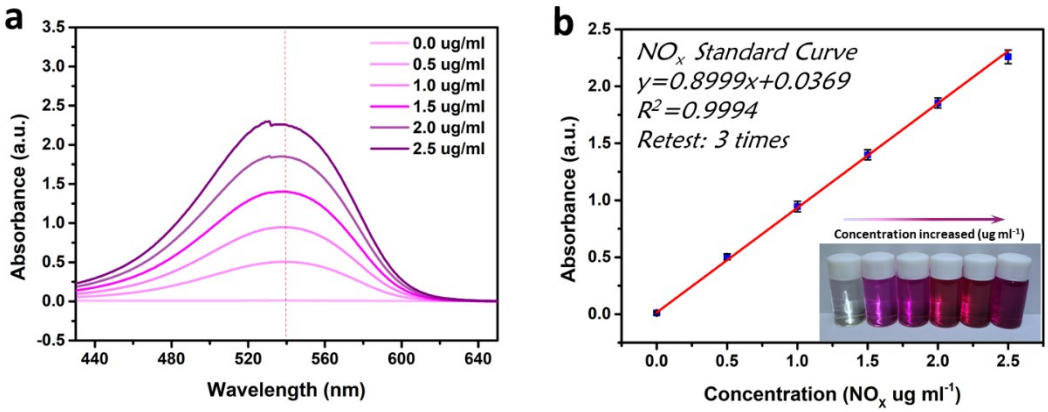

Figure S13. Determination of the NO_x in 0.1 M Na_2SO_4. (a) UV-Vis absorption spectra of various NO_x concentrations after incubated for 20 min at room temperature. (b) Corresponding calibration curves for the colorimetric NO_x assay using the N-(-1-naphthyl) ethylenediamine dihydrochloride spectrophotometric method.

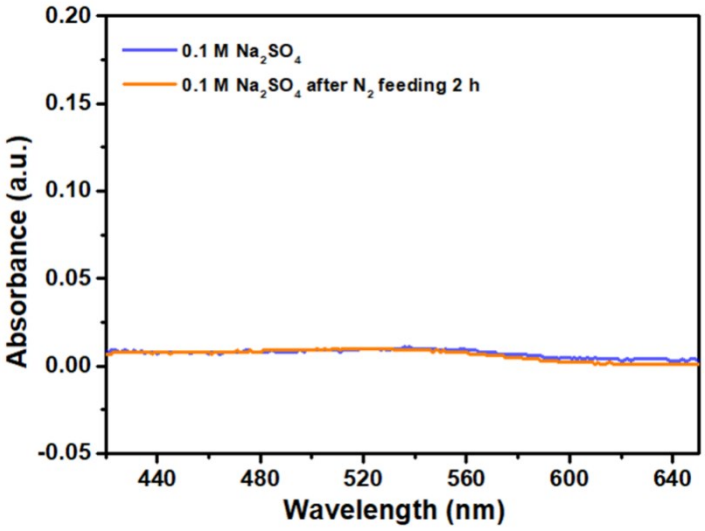

144

145 **Figure S14.** The UV-Vis absorption spectra of the 0.1 M Na_2SO_4 background and the
146 purified N_2 treated 0.1 M Na_2SO_4 solution using an N-(-1-naphthyl) ethylenediamine
147 dihydrochloride spectrophotometric method. The results show that no NO_x exists in the
148 purified gas.

149

150

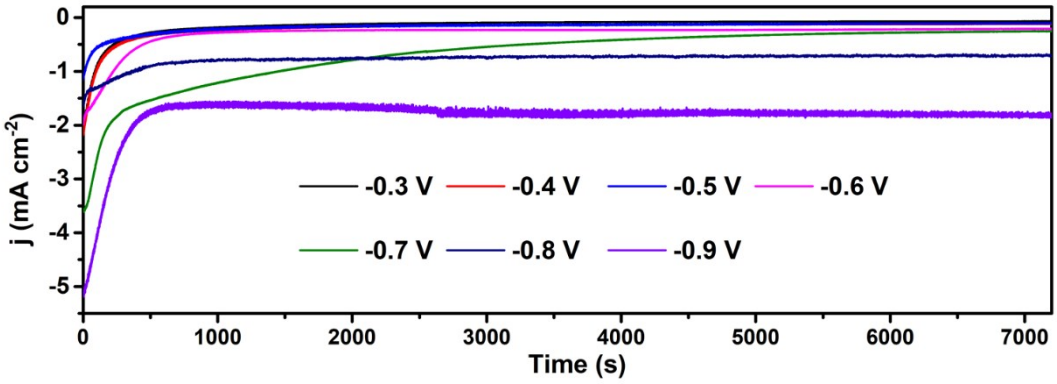

151

152

153 **Figure S15.** Time-dependent current density curves for SnS@C at the corresponding
154 different potentials for 7200 s in 0.1 M Na_2SO_4 solution.

155

156

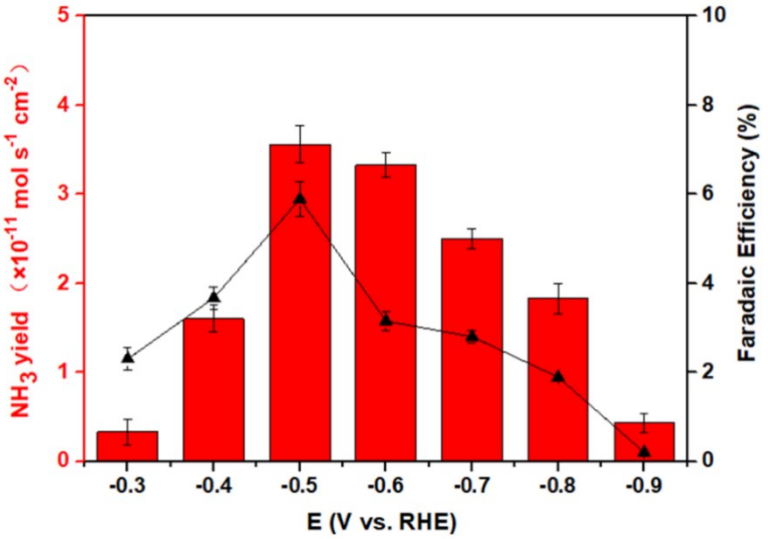

157

158 **Figure S16.** NH_3 yield rates and FEs of SnS at a series of potentials.

159

160

161

162

163

164

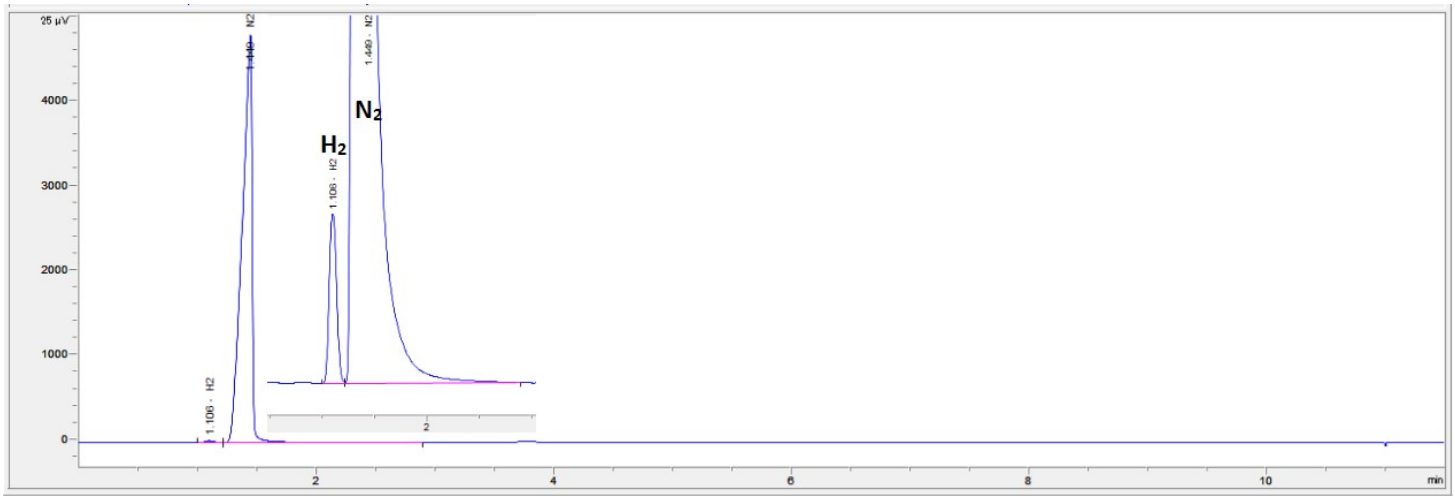

165

166 **Figure S17.** Gas chromatography spectra showing the detection of CO and H_2.

167

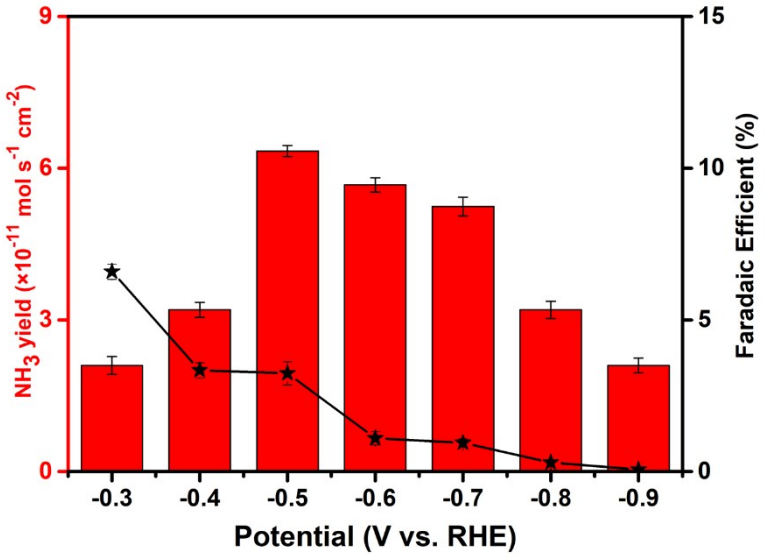

168

169 **Figure S18.** NH_3 yield rates and FE of SnS@C at various potentials in 0.1 M HCl.

170

171

172

173

174

175

176

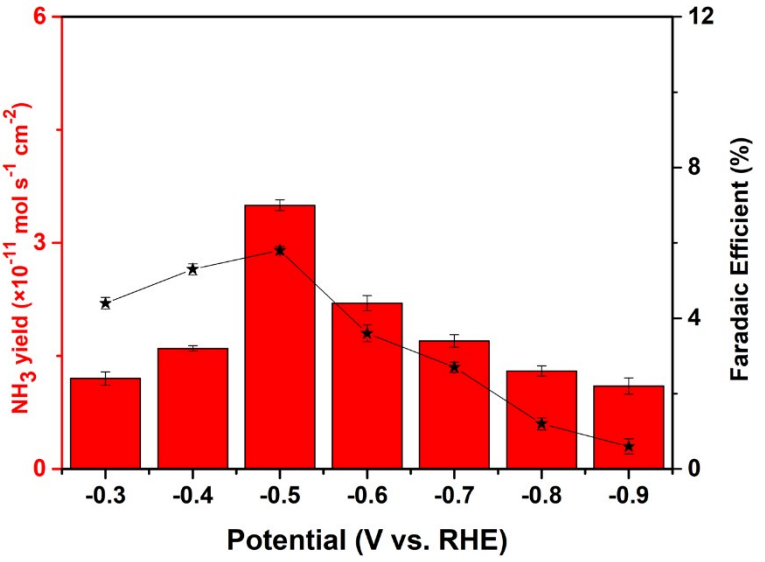

177

Figure S19. NH_3 yield rates and FE of SnS@C at various potentials in 0.1 M KOH.

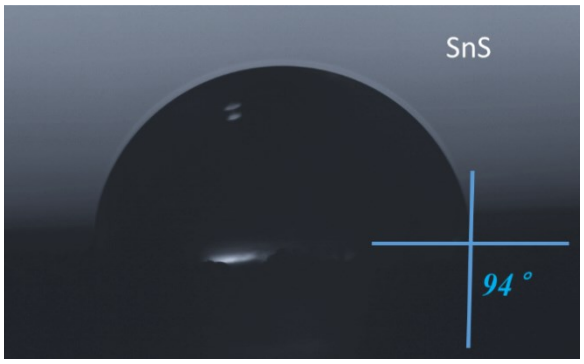

Figure S20. The electrolyte contact angle measurements of SnS.

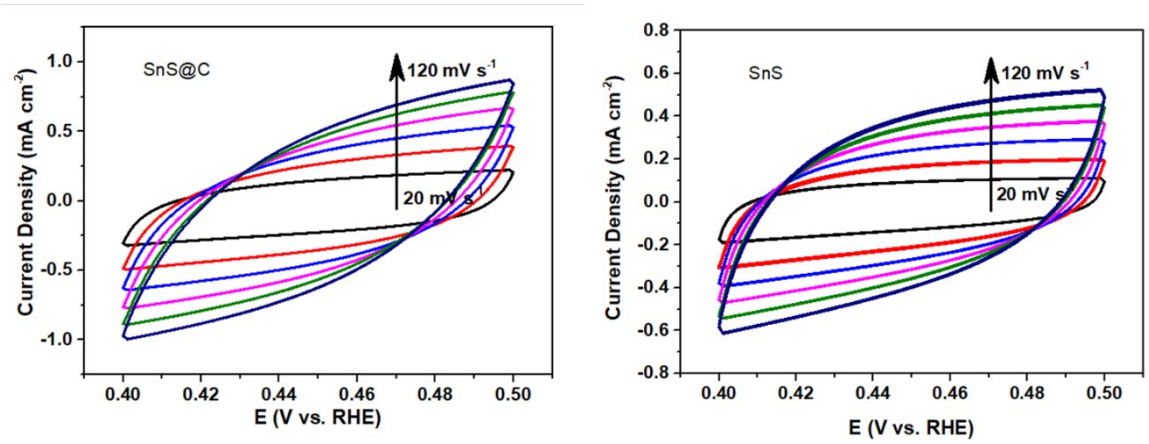

Figure S21. The CV curves of SnS@C and SnS collected at different scanning rates from 20 to 120 mV s^{-1}.

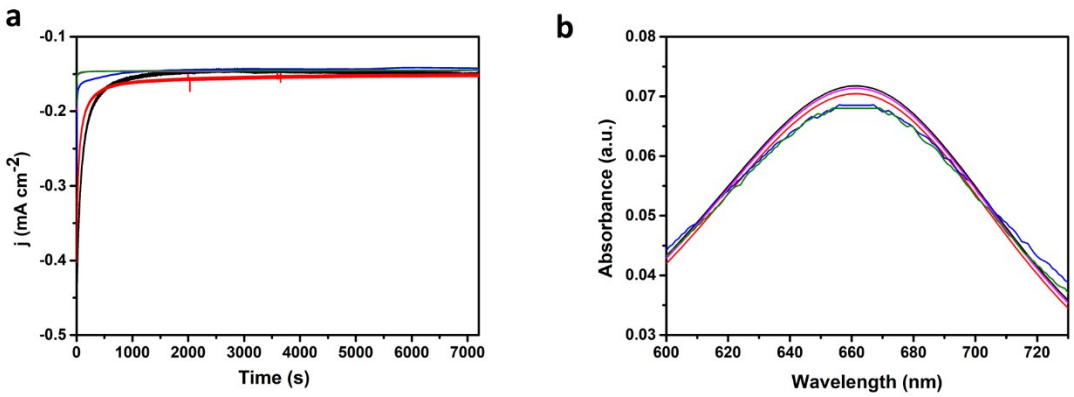

Figure S22. Five consecutive NRR electrolysis cycles at –0.50 V (vs. RHE) for 7200s in a 0.1 M Na_2SO_4 solution. (a) Time-dependent current density curves of SnS@C. (b) UV-Vis absorption spectra of the electrolytes stained with the indophenol blue method (obtained by repeating electrolysis 5 times).

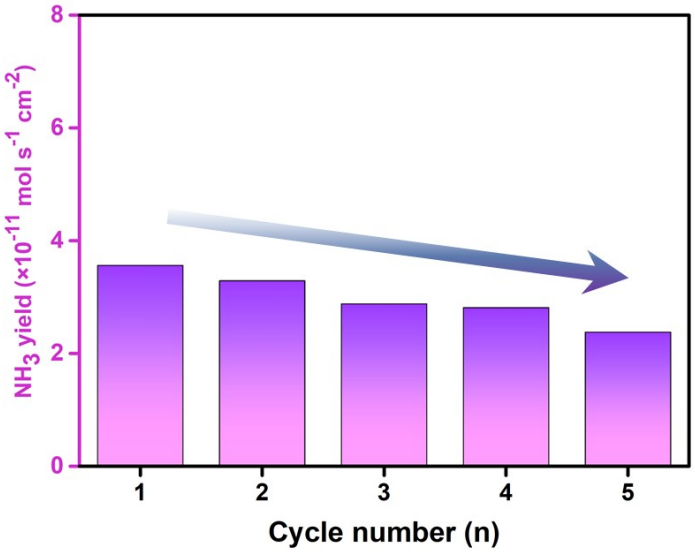

Figure S23. Recycling performances of SnS at –0.50 V (vs. RHE).

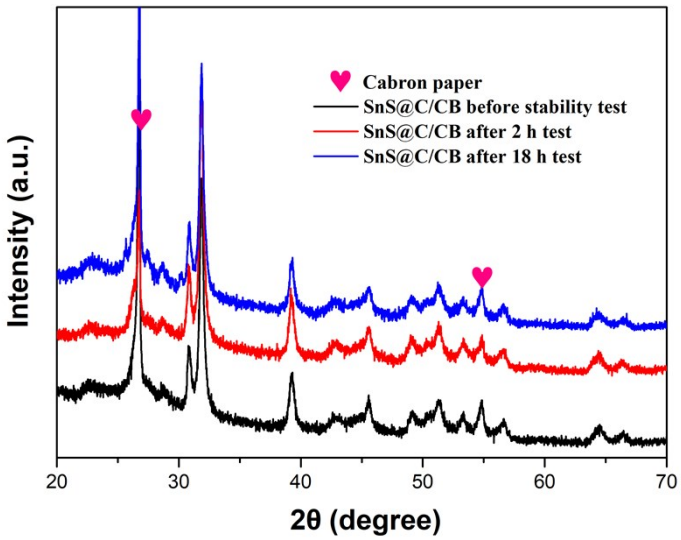

209 **Figure S24.** XRD pattern of SnS@C before and after stability test.

210

211

212

213

214

215

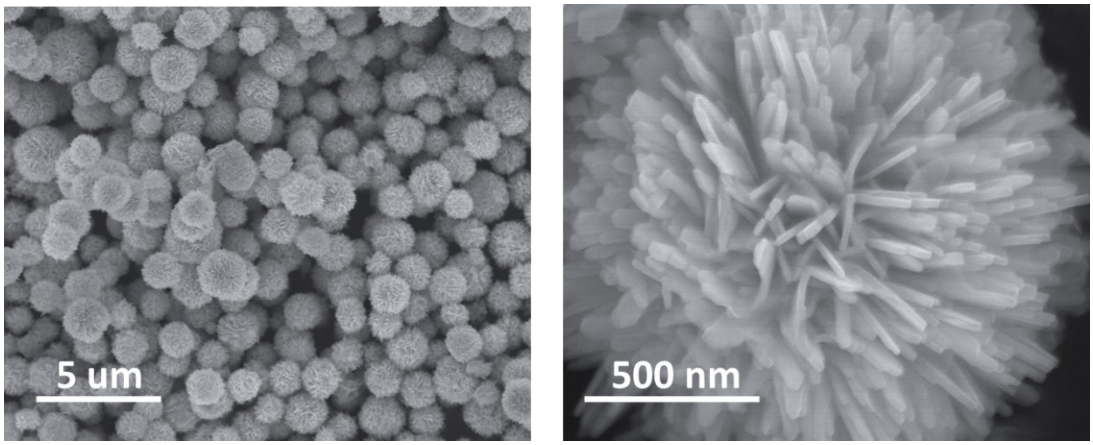

216 **Figure S25.** SEM images of SnS@C after stability test.

217

218

219

220

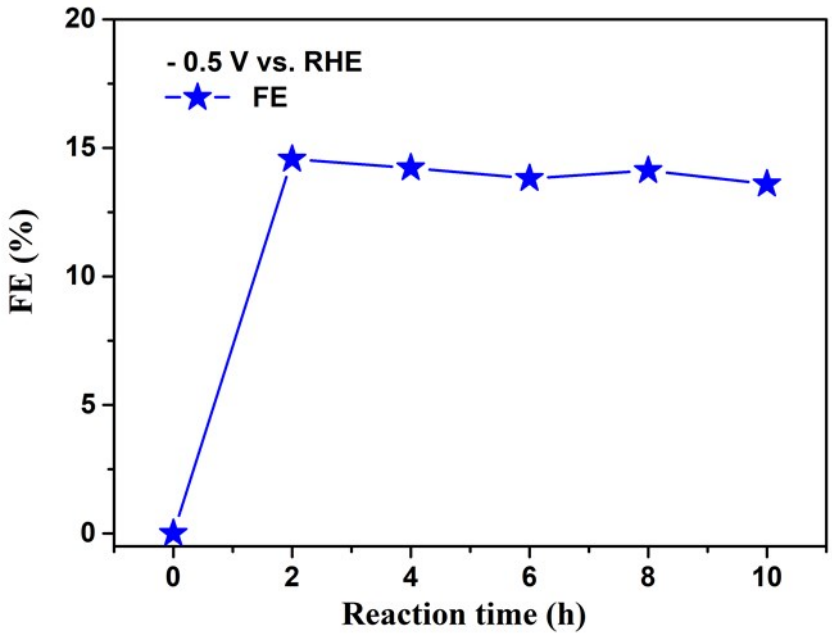

221

222 **Figure S26.** The FE of SnS@C vs. reaction time at -0.5 V.

223

224

225

226

227

228

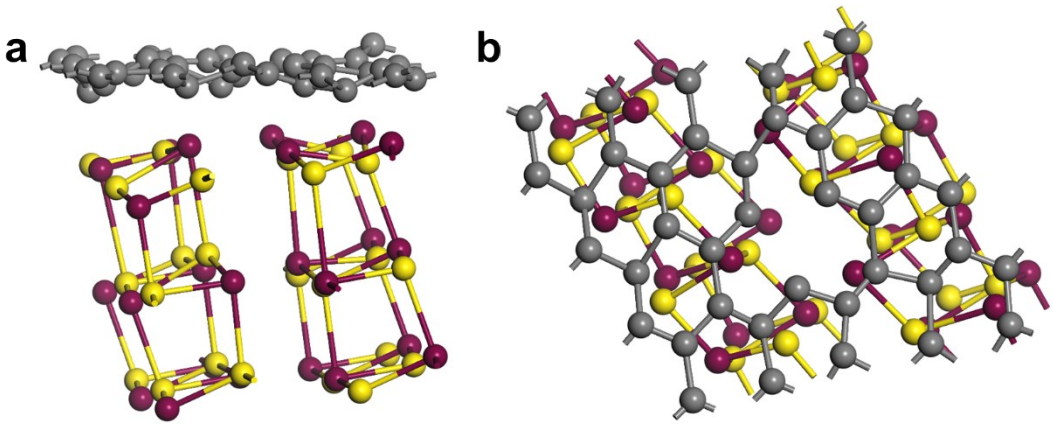

229 **Figure S27.** a) The structure diagram of SnS@C; b) Top view of SnS@C (The gray,
230 chocolate and yellow balls represent C, Sn, and S, respectively)

231

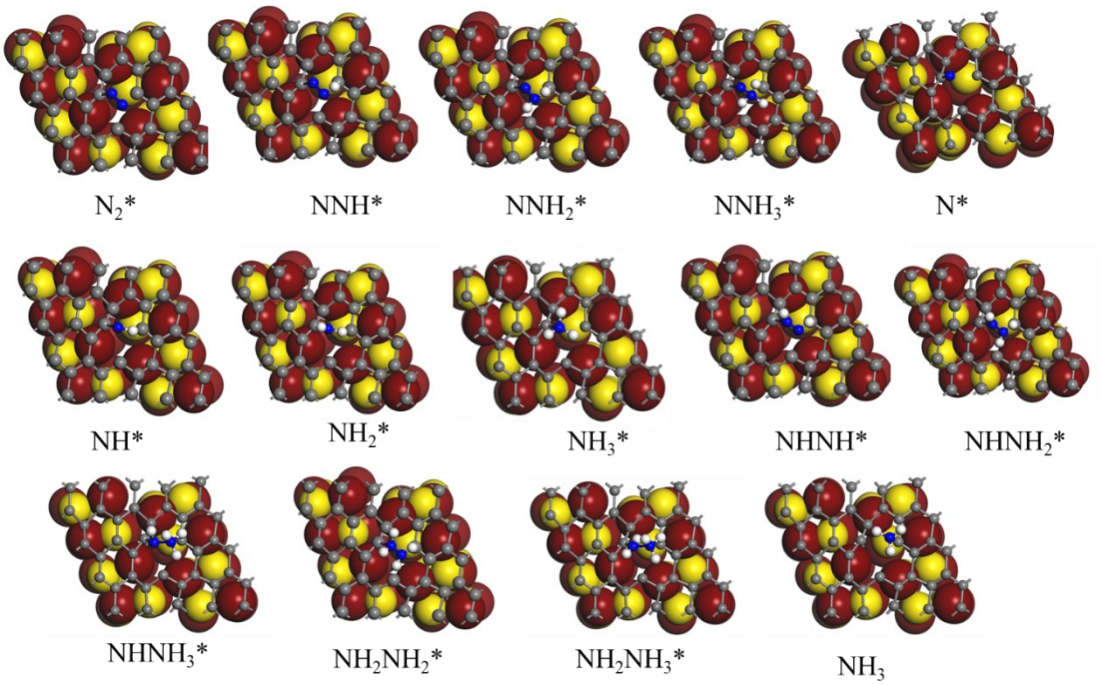

Figure S28. Space-filling geometric structures of various intermediates of the NRR pathway on the SnS@C (111) surface. (The gray, white, blue, chocolate and yellow balls represent C, H, N, Sn and S, respectively)

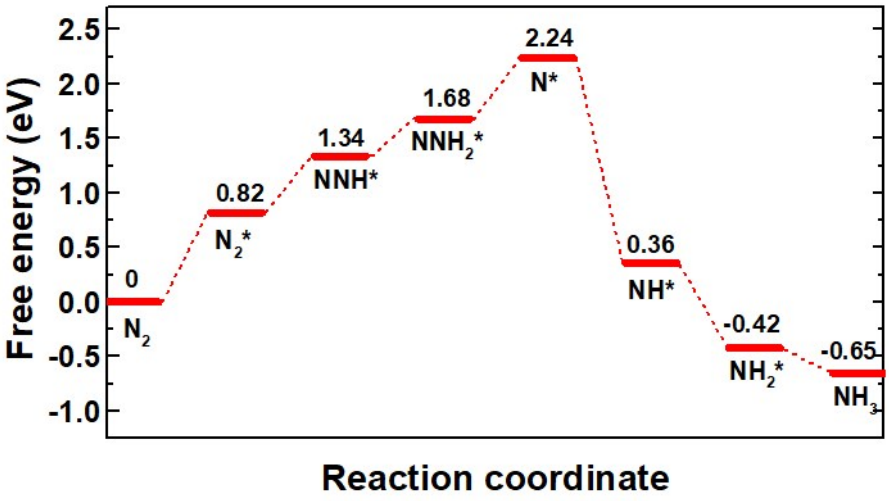

242

243 **Figure S29.** Free-energy diagrams of NRR process on SnS (111) surface (* denotes the
244 adsorption site)

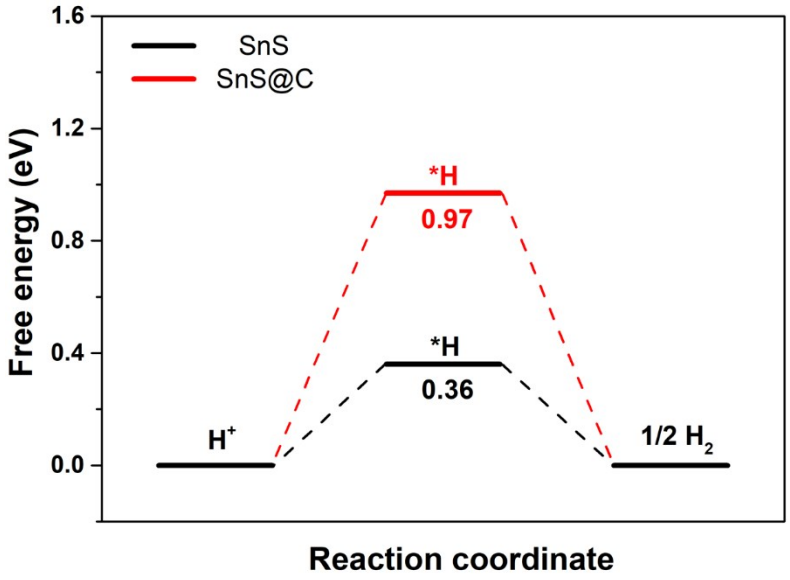

245

246 **Figure S30.** Free-energy diagrams of HER process on SnS and SnS@C (* denotes the
247 adsorption site).

248

249

250

251

252

253

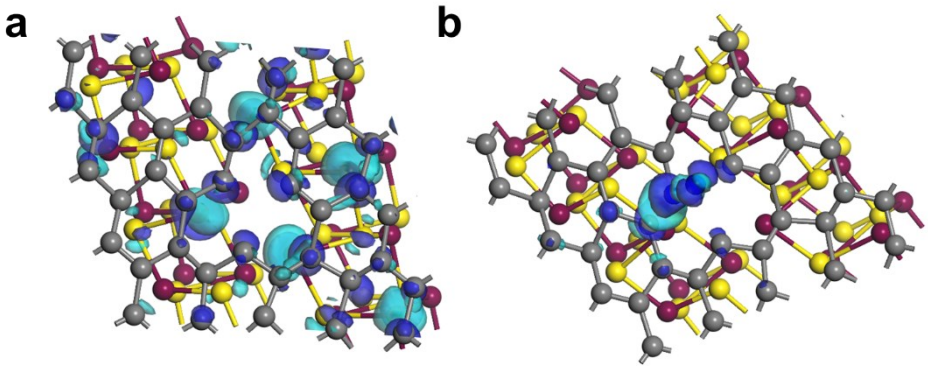

Figure S31. Top view of a) Charge density difference of SnS@C; b) Charge density difference of SnS@C after N_2 adsorption on SnS (111) surface. (Wathet and mazarine blue isosurfaces represent charge accumulation and depletion, respectively)

	ZPE (eV)	$\int C_P dT$ (eV)	-TS (eV)
*NNH	0.50	0.06	-0.10
*NNHH	0.77	0.09	-0.18
*N	0.09	0.02	-0.03
*NH	0.39	0.03	-0.04
*NHH	0.65	0.04	-0.07
NH_3	0.85	0.10	-0.60
N_2	0.14	0.09	-0.40
H_2	0.27	0.09	-0.42

Table S1. The correction of zero-point energy, enthalpy effect, and entropy effect of the adsorbed and gaseous species.

Samples	SnS	SnS@C
m_s/m_{Sn}[a]	0.286	0.285
n_s/n_{Sn}[a]	1.05	1.03
n_s/n_{Sn}[b]	1.13	1.08
Sn^{4+}/Sn^{2+}	1.88	0.74

271

272 m_s/m_{Sn} is the mass ratio of the S and Sn on SnS and SnS@C;

273 n_s/n_{Sn} is the molar ratio of S and Sn elements on SnS and SnS@C;

274 [a] Results measured by EDX analysis;

275 [b] Results measured by XPS analysis.

276 **Table S2.** Chemical compositions of SnS and SnS@C

277

278

Samples	C %		H %		S %	
	before tests	after tests	before tests	after tests	before tests	after tests
SnS	4.2	4.26	0.84	0.94	21.68	20.86
SnS@C	7.07	7.14	1.15	1.22	20.8	20.62

279 **Table S3.** Chemical composition determined by an elemental analyzer.

280

281

282

Samples	R_s/Ω	R_{ct}/Ω
SnS	78.73	236.48
SnS@C	34.57	120.25

283 **Table S4.** Simulated values of fitted equivalent circuit resistances of SnS and SnS@C.

Catalyst	System	NH_3 yield rate	FE (%)	References
SnS@C microflowers	0.1 M Na_2SO_4	7.95×10^{-11} mol s^{-1} cm^{-2}	14.56	**This work**
Sn/SnS nanosheets	0.1 M PBS	3.89×10^{-11} mol s^{-1} cm^{-2} (-0.8V)	6.5 (-0.7V)	**1**
SnO_2/RGO	0.1 M Na_2SO_4	8.33×10^{-11} mol s^{-1} cm^{-2}	7.1	**2**
Sn dendrite/Sn foil	0.1 M PBS	5.66×10^{-11} mol s^{-1} cm^{-2}	3.67	**3**
NiCoS/C	0.1 M Li_2SO_4	2.60 ug h^{-1} cm^{-2}	12.9	**4**
Co-$FePS_3$ nanosheets	0.1 M KOH	90.6 ug h^{-1} mg_{cat}^{-1} (0.04 mg)	3.38	**5**
Fe-MoS_2/CC	0.1 M KOH	12.5 ug h^{-1} cm^{-2}	10.8	**6**
FeS_2	0.1 M Na_2SO_4	37.2 ug h^{-1} mg_{cat}^{-1} (0.2 mg)	11.2	**7**
CoS_2@NC/CP	0.1 M HCl	17.45 ug h^{-1} mg_{cat}^{-1} (0.1 mg)	4.6	**8**
Porous Au film	0.1 M Na_2SO_4	9.42 ug cm^{-2} h^{-1}	13.36	**9**
WS_2/WO_2	0.05 M H_2SO_4	8.53 ug h^{-1} mg_{cat}^{-1} (0.02 mg)	13.5	**10**
Ni-Fe@MoS_2	0.1 M Na_2SO_4	128.17 ug h^{-1} mg_{cat}^{-1} (0.05 mg)	11.34 (40 ℃)	**11**
Pd-Ag-S	0.1 M Na_2SO_4	9.73 ug h^{-1} mg_{cat}^{-1} (0.1 mg)	18.41	**12**
MoS_2-rGO/CP	0.1 M $LiClO_4$	24.82 ug h^{-1} mg^{-1}	4.58	**13**
Ag_3Cu BPNs	0.1 M Na_2SO_4	9.84 ug h^{-1} cm^{-2}	13.28	**14**
PTCA-rGO	0.1M HCl	24.7 ug h^{-1} mg^{-1}	6.9	**15**

Mn_3O_4	0.1 M Na_2SO_4	11.6 ug h^{-1} mg^{-1}	3.0	**16**
FePc/C	0.1 M Na_2SO_4	137.95 ug mg_{FePc}^{-1} h^{-1}	10.5	**17**

285

286 **Table S5.** The comparable table of state-of-the-art NRR catalysts.

287

288

Reference

1. P. Li, W. Fu, P. Zhuang, Y. Cao, C. Tang, A. B. Watson, P. Dong, J. Shen and M. Ye, *Small*, 2019, **15**, e1902535.

2. K. Chu, Y.-p. Liu, Y.-b. Li, J. Wang and H. Zhang, *ACS Applied Materials & Interfaces*, 2019, **11**, 31806-31815.

3. X. Lv, F. Wang, J. Du, Q. Liu, Y. Luo, S. Lu, G. Chen, S. Gao, B. Zheng and X. Sun, *Sustainable Energy & Fuels*, 2020, DOI: 10.1039/d0se00828a.

4. X. Wu, Z. Wang, Y. Han, D. Zhang, M. Wang, H. Li, H. Zhao, Y. Pan, J. Lai and L. Wang, *Journal of Materials Chemistry A*, 2020, **8**, 543-547.

5. H. Huang, F. Li, Q. Xue, Y. Zhang, S. Yin and Y. Chen, *Small*, 2019, **15**, e1903500.

6. X. Zhao, X. Zhang, Z. Xue, W. Chen, Z. Zhou and T. Mu, *Journal of Materials Chemistry A*, 2019, **7**, 27417-27422.

7. H. Du, C. Yang, W. Pu, L. Zeng and J. Gong, *ACS Sustainable Chemistry & Engineering*, 2020, **8**, 10572-10580.

8. P. Wei, H. Xie, X. Zhu, R. Zhao, L. Ji, X. Tong, Y. Luo, G. Cui, Z. Wang and X. Sun, *ACS Sustainable Chemistry & Engineering*, 2019, **8**, 29-33.

9. H. Wang, H. Yu, Z. Wang, Y. Li, Y. Xu, X. Li, H. Xue and L. Wang, *Small*, 2019, **15**, 1804769.

10. Y. Ling, F. M. D. Kazim, S. Ma, Q. Zhang, K. Qu, Y. Wang, S. Xiao, W. Cai and Z. Yang, *Journal of Materials Chemistry A*, 2020, **8**, 12996-13003.

11. L. Zeng, X. Li, S. Chen, J. Wen, W. Huang and A. Chen, *Journal of Materials Chemistry A*, 2020, **8**, 7339-7349.

12. H. Wang, S. Liu, H. Zhang, S. Yin, Y. Xu, X. Li, Z. Wang and L. Wang, *Nanoscale*, 2020, **12**, 13507-13512.

13. X. Li, X. Ren, X. Liu, J. Zhao, X. Sun, Y. Zhang, X. Kuang, T. Yan, Q. Wei and D. Wu, *Journal of Materials Chemistry A*, 2019, **7**, 2524-2528.

14. H. Yu, Z. Wang, D. Yang, X. Qian, You. Xu, X. Li, H. Wang, L. Wang, *Journal of Materials Chemistry A,* 2019, **7**, 20, 12526-12531.

15. P. Li, J. Wang, H. Chen, X. Sun, J. You, S. Liu, Y. Zhang, M. Liu, X. Niu and Y. Luo, *Journal of Materials Chemistry A*, 2019, **7**, 12446-12450.

16. X. Wu, L. Xia, Y. Wang, W. Lu, Q. Liu, X. Shi and X. Sun, *Small*, 2018, **14**, e1803111.

17. C. He, Z.-Y. Wu, L. Zhao, M. Ming, Y. Zhang, Y. Yi and J.-S. Hu, *ACS Catalysis*, 2019, **9**, 7311-7317.